Load-controlled cyclic T-bar tests:

a new method to assess the combined effects of cyclic loading and consolidation

Manuscript submitted to Géotechnique Letters

C. D. O'Loughlin, Z. Zhou, S. A. Stanier and D. J. White

Conleth D. O'LOUGHLIN
Centre for Offshore Foundation Systems and ARC Research Hub for Offshore Floating Facilities
University of Western Australia
Perth, WA 6009, Australia
Tel: +61 8 6488 7326
Email: conleth.oloughlin@uwa.edu.au

Zefeng ZHOU (corresponding author)
Centre for Offshore Foundation Systems and ARC Research Hub for Offshore Floating Facilities
University of Western Australia
Perth, WA 6009, Australia
Tel: +61 403848151
Email: zefeng.zhou@research.uwa.edu.au

S. A. STANIER
University of Cambridge and ARC Research Hub for Offshore Floating Facilities
Cambridge CB2 1PZ, UK
Tel: +44 7856 009042
Email: sas229@cam.ac.uk

David J. WHITE
University of Southampton and ARC Research Hub for Offshore Floating Facilities
Southampton, Southampton SO17 1BJ, UK
Tel: +44 23 8059 6859
Email: david.white@soton.ac.uk

Number of words (excluding abstract, acknowledgements, references, tables and figure captions): 2620
Number of tables: 2
Number of figures: 9

Load-controlled cyclic T-bar tests:
A new method to assess the combined effects of cyclic loading and consolidation

C. D. O'LOUGHLIN[1], Z. ZHOU[2], S. A. STANIER[3] AND D. J. WHITE[4]

Full-flow T-bar and ball penetrometer tests are often used to measure intact and remoulded soil strengths, with the latter determined after several large amplitude displacement cycles. In offshore design the remoulded soil strength is often the governing design parameter during installation of subsea infrastructure, whilst a 'cyclic strength' applies for the less severe operational cyclic loading. This paper utilises T-bar penetrometer tests to measure both remoulded and cyclic strengths, where the latter is determined via a new test protocol involving cycles between load rather than displacement limits. The tests use kaolin clay and a reconstituted carbonate silt and involve three cyclic phases with intervening consolidation periods. The results demonstrate the important and beneficial role of consolidation, with the loss in strength due to remoulding sometimes surpassed by the strength recovery from consolidation. The most significant gains in strength, to 2.5 times the initial value, were measured in the load-controlled cyclic tests. These data demonstrate a novel way to characterise undrained cyclic strength, taking advantage of consolidation to reduce conservatism.

Keywords: penetrometer, soil strength, cyclic loading, soil strength, consolidation and remoulding.

[1] *Centre for Offshore Foundation Systems, The University of Western Australia, Crawley, WA 6009, Australia*
[2] *Centre for Offshore Foundation Systems, The University of Western Australia, Crawley, WA 6009, Australia (Corresponding author: Email: zefeng.zhou@research.uwa.edu.au)*
[3] *University of Cambridge, Cambridge CB2 1PZ, UK*
[4] *University of Southampton, Southampton SO17 1BJ, UK*

INTRODUCTION

Offshore foundations are subject to cyclic loading from the ocean environment and from operational loads, such as expansion and contraction of pipelines. In conventional design, cyclic loading of fine-grained soils is treated as 'damage', so the cyclic undrained shear strength is less than the monotonic value at the same strain rate. The severity of the 'damage' is governed by the magnitude and number of cycles, and whether the loading is one-way or two-way. Procedures to estimate design cyclic strengths are based on contour diagrams of shear strain or excess pore pressure (e.g. Andersen et al. 1988, Andersen 2015). Although this methodology is well-established and robust, it neglects the potential for regains in soil strength associated with dissipation of the excess pore pressure induced by the cyclic loads.

Ignoring the regain in strength due to dissipation of excess pore pressures can result in a conservatively low estimate of soil strength, if in practice some dissipation will occur prior to the governing load being applied. This recovery is illustrated by the model scale T-bar penetrometer test in soft kaolin clay shown in Figure 1 (Hodder et al. 2013), which involved episodes of undrained cycling interspersed with consolidation periods. Although the strength degrades within each episode, the regain from consolidation is significant. This example represents onerous cyclic loading, such as that caused by an oscillating catenary riser pipe where it touches down on the seabed. Another example in which consolidation-induced strength gain is increasingly recognised, and considered in design, is the soil strength and axial friction beneath on-bottom pipelines. Experimental and numerical modelling shows that cyclic loading as a pipe is laid on the seabed causes a loss of strength due to remoulding, but the consolidation process leads to higher friction in the long term (White et al. 2017).

Previous evidence of this behaviour has been limited to clays of low sensitivities. Natural offshore clays are typically more sensitive, which raises the question of whether the potential for strength regain is as significant in these soils. Other offshore cyclic loading scenarios are also less severe, such as one-way cyclic loading of an anchor. In this case the cyclic loads do not exceed the monotonic capacity, in contrast to the soil flow during large amplitude cycles of a T-bar, which strains the soil beyond failure. The regain in soil strength from this lower-amplitude cycling has received less attention, despite its higher relevance for most offshore design problems.

This paper addresses these knowledge gaps through an experimental study of changes in undrained shear strength from mild and severe cyclic loading and consolidation, applied via a

T-bar penetrometer.

PENETROMETER TESTS

The tests used normally consolidated kaolin clay and carbonate silt with properties given in Table 1. Both soils were consolidated from a slurry. To vary the sensitivity of the kaolin clay, two further slurry batches were prepared with the addition of a dispersant (Sodium Hexametaphosphate) and a flocculant (Sodium Polyacrylate). These additives raise the initial voids ratio of the kaolin clay during consolidation by encouraging groups of particles to coalesce together into effectively larger particles (Bergaya et al. 2006). As shown later, the concentrations were varied in the two 'modified' batches, which had the effect of raising the soil sensitivity from S_t = 2.5 (unmodified kaolin clay) to S_t = 4.5 and S_t = 6.5 (see Table 1). The experimental programme involved both single gravity and centrifuge tests. The single gravity samples were consolidated in tubes with a specific surcharge plate to accommodate the penetrometer (Suzuki 2015, Colreavy et al. 2019) whereas the centrifuge experiments were conducted at an acceleration of 150g in rectangular sample containers (Figure 2).

All samples were normally consolidated, which was achieved by self-weight consolidation for the centrifuge samples (at 150g) and by increasing the oedometric consolidation pressure to a vertical stress of σ'_{v0} = 48 kPa for the single gravity tests.

The T-bar penetrometer uses a cylindrical bar, 5 mm in diameter and 20 mm in length, connected perpendicularly to a 5 mm diameter shaft. Strain gauges are located on a thin-walled section near the base of the shaft to measure penetration and extraction resistance. Each penetrometer test involved penetration to a target depth followed by cyclic sequences, undertaken in either displacement or load control, interspersed with consolidation periods during which the T-bar was held at a fixed displacement (see Table 2 and Figure **3** for details). The displacement controlled cycles involved moving the T-bar vertically by ± 4 or 4.5 diameters for N = 20 cycles, whereas the load controlled cycles were undertaken between load limits that mobilised either 0% and 75% or 25% and 75% of the intact penetration resistance (and therefore the initial undrained shear strength, $s_{u,i}$) for either N = 20 or 1080 cycles.

Consolidation periods, t_c = 1 and 2.5 hours for the silt and kaolin respectively, were included in the centrifuge cyclic loading sequences. A longer consolidation period, t_c = 24 hours was used in the single gravity tests. A penetration velocity, v_p = 3 mm/s and a loading frequency of 1 or 5 Hz were adopted for the displacement and load-controlled cycles respectively. A penetration velocity, v_p = 3 mm/s was selected to ensure that the response was primarily undrained, noting that the dimensionless group, v_pD/c_h = 53 (where D is the T-bar diameter), in excess of the v_pD/c_h > 10 criteria for undrained behaviour (e.g. Lehane et al. 2009, Colreavy et al. 2016). A loading frequency of 1 or 5 Hz was adopted for the load-controlled cycles to strike a balance between achieving the targeted undrained response and ensuring accurate load limit control. Undrained shear strength was calculated as $s_u = q/N_{T\text{-bar}}$, where q is the measured penetration resistance (i.e. the gross pressure on the T-bar projected area) and $N_{T\text{-bar}}$ is the T-bar bearing factor, taken as 10.5 (Martin and Randolph, 2006).

EFFECT OF SOIL SENSITIVITY ON CONSOLIDATION-INDUCED STRENGTH REGAIN

Figure 4a shows profiles of undrained shear strength, s_u, with depth, z, for the single gravity Type II tests in kaolin clay with different sensitivities (Tests 1-3). Adding flocculants to the kaolin clay increased the intact strength, while the remoulded strength remaining approximately constant. Sahdi et al. (2010) saw a similar response for kaolin clay with coloured dye. Sensitivity, S_t, defined as the ratio of intact to fully remoulded strength in the first cyclic episode, was S_t = 2.5 for pure kaolin but up to 6.5 for samples with additives. The corresponding undrained shear strength ratios, $(s_{u,i}/\sigma'_{v0})_{NC}$ are 0.15 and 0.4.

After the t_c = 24 hour consolidation period between each episode, s_u increases due to dissipation of the excess pore pressure from the preceding cycles. During the first consolidation period strength increases by a factor of 2.6 - 4.6, and during the second period by a factor of 1.9 - 2.5 (Figure 4b). The greater gains are for the soils with higher sensitivity, indicating that the potential for consolidation-induced strength gain is actually higher in soils with increased sensitivity.

The changes in strength, expressed relative to the initial strength, $s_{u,i}$, for pure kaolin and the carbonate silt show similar trends (Figure 5). The carbonate silt has a higher sensitivity, so the cyclic sequences soften more. However, the proportional gain in strength during each consolidation period is also higher for the carbonate silt.

These responses can be illustrated conceptually via the stress path of a soil element during and after cyclic remoulding for soils of low and high sensitivity (Figure 6). The elements for a low and a high sensitivity soil are assumed to start at the same state on a normal compression line (NCL) (Point O in Figure 6). Initial penetration of the T-bar induces excess pore pressures that reduce the vertical effective stress from point O to point A. Cycling the T-bar generates additional excess pore pressure until the stress reaches the fully remoulded strength line (RSL) at point B (White and Hodder 2010; Hodder et al. 2013; Zhou et al. 2019).

The distance between the NCL and the RSL is controlled by the sensitivity, such that the fully remoulded state for a low sensitivity soil is represented by point B_1, which is at a higher vertical effective stress than for a high sensitivity soil, which is represented by point B_2. The reconsolidation phase follows a stress path shown by the κ line. After consolidation the reduction in specific volume, v, and hence the increase in s_u, is higher for the higher sensitivity soil (point C_2) than for the low sensitivity soil (point C_1). This analysis matches the test results, and is intended to indicate only the relative positions of the NCL and RSL. In practice, both may move due to the level of structure in the soil, as evident from the higher intact strengths in the higher sensitivity kaolin in Figure 4. However, the relative changes in strength are controlled by the relative spacing of the (normal and remoulded compression) lines, not their absolute position.

EFFECT OF ONE-WAY CYCLIC LOADING ON SOIL STRENGTH

The Type III tests involved penetration to 43 mm depth followed by 20 load-controlled cycles between $0.25q_i$ and $0.75q_i$, where q_i was the initial resistance at that depth. After the cycles, penetration either resumed immediately (Test 6a, Figure 7a) or after consolidation for t_c = 2.5 hours (Test 6b, Figure 7b). A reference test without cycling is also shown on Figure 7. The cycles alone have negligible effect on s_u (Figure 7a) but after consolidation there is a localised increase in s_u to ~$2.2s_{u,i}$.

The changes in s_u from all Type III tests (Tests 6a-e, Tests 9a-e) with small-amplitude load-controlled cycles are summarised in Figure 8, alongside the large-amplitude cyclic tests (Type IV), with a sub-figure for each soil type. The following observations are made:

- The displacement-controlled cycles fully remould the soil causing a significant reduction in strength. In contrast, the load-controlled cycles cause minimal reduction in soil strength (<5%), even though each cycle mobilises $0.75s_{u,i}$.

- The increase in s_u after the consolidation period following each load-controlled cyclic episode is significant for both soils. Strengths of $2.1s_{u,i}$ and $2.5s_{u,i}$ are reached after the first and second consolidation periods in kaolin, compared to $2.0s_{u,i}$ and $2.3s_{u,i}$ in the carbonate silt. These post-consolidation strengths are typically 2-3 times greater than observed after the displacement-controlled cycles.

- Consolidation immediately following the initial penetration (i.e. without load cycles, Test Type I) also led to a significant increase in s_u, to ~$1.9s_{u,i}$ for kaolin (Test 4) and ~$1.7s_{u,i}$ for carbonate silt (Test 7). However, a greater strength is measured when the consolidation period is preceded by a cyclic episode, which generates additional excess pore pressure.

- Tests 10 and 11 provide further evidence of the gain in strength from combined cyclic loading and consolidation. These Type IV tests (Figure 3d) involved N = 1,080 cycles in a single episode (reflecting the number of cycles that might occur in a typical three-hour storm). There was no subsequent consolidation period but consolidation would have occurred concurrent with the cycles. This process caused s_u to increase by 2.35 times in Test 10 (which cycled from $0.25q_i$ - $0.75q_i$), and by 2.9 times in Test 11 (which cycled from 0 - $0.75q_i$). These increases are slightly higher than the strength gain from three N = 20 cyclic episodes with intervening t_c = 1 hour consolidation periods.

Figure 8 highlights the range of changes in soil strength that can result from cyclic loading; the variation from fully remoulded conditions to the consolidation-induced hardening after one-way cyclic loading is a factor of 6 for kaolin clay and 11.5 for the carbonate silt.

These varying changes in strength can also be explained using conceptual stress-paths for each Test Type. For example, the first episode of one-way cyclic loading followed by consolidation (Type III) is represented in Figure 9a by the stress path O-A_2-B_2, which generated more excess pore pressure than Type I (O-A_1-B_1) as Type III involved 20 cycles of one-way loading after the initial penetration. During the subsequent consolidation, the reduction in specific volume for Type III (Δv_{III}) is higher than that for Type I (Δv_I), so the potential for further excess pore pressure generation (e.g. in the next T-bar pass, stress paths A_1-B_1 and A_2-B_2) is lower for Type III than Type I. Consequently, the next pass of the T-bar involves a higher vertical effective stress and soil strength for Type III (point B_2) than Type I (point B_1).

The same logic applies to Type IV; the additional cycles (N = 1080) generate additional pore pressure, although concurrent consolidation leads to a curved effective stress path. The pore pressure generation increases with cyclic amplitude so the reduction in specific volume is higher for Test IV-b (0 - $0.75q_i$, $\Delta v_{IV\text{-}b}$) than Test IV-a ($0.25q_i$ - $0.75q_i$, $\Delta v_{IV\text{-}a}$), leading to a higher strength gain.

Figure 9b compares stress paths for a soil element subjected to 20 displacement- and load-controlled cycles followed by the same consolidation period. The displacement-controlled cycles in Type II led to fully remoulded conditions and hence a low vertical effective stress on the RSL, whereas the load-controlled cycles generated much less excess pore pressure so the post-cyclic effective stress was higher. Hence, after consolidation the reduction in specific volume is greater for Type II (Δv_{II}) than Type III (Δv_{III}), so the remobilised soil strength is higher for Type II than Type III, whereas Figure 8b shows the opposite. However, if the very high accumulated shear strain causes the intact strength line (ISL) to migrate to the left (e.g. as per the models of Cocjin et al. 2017; Hodder et al. 2013; Zhou et al. 2019), then the effective stress and soil strength in Type II (point B_5) is lower than in Type III (point B_2).

Across all of the test types, the gain in strength relative to the initial strength is converging towards $s_u/s_{u,i}$ ~ 3-4. Similar evidence is provided by other studies using variable rate and episodic penetrometer tests (Chow et al. 2019). This value is similar to the spacing ratio between the intact and remoulded or critical state lines, which controls the gain in strength predicted from these critical state-type frameworks. Parallel work for the axial friction on pipelines and shallow penetrometers shows that the undrained strength of normally-consolidated soil can rise by this ratio under episodes of sliding failure and reconsolidation (White et al. 2015, Schneider et al. 2019). The present study suggests that the same ratio may be generally applicable for bearing-type loading.

CONCLUSIONS

The changing strength of soft soil when subjected to varying episodes of cyclic loading is a topical challenge in offshore engineering.

Data from T-bar penetrometer tests involving episodes of large amplitude cyclic displacements and also novel small-amplitude load cycling highlights the effect of consolidation on strength. Large amplitude cyclic loading remoulds the soil to a minimum value, although the regain in strength due to consolidation is significant, and can surpass the strength loss from remoulding. The regain is higher in soils with higher sensitivities. Low amplitude one-way cyclic loading, mobilising a peak resistance equivalent to 75% of the initial monotonic strength, did not cause a reduction in strength, but led to a very significant increase in soil strength, to almost 2.5 times the initial monotonic strength, due to the consolidation either during or after cycling.

Consolidation around a T-bar penetrometer is relatively rapid due to the small device, which allows these new test protocols to explore changes in strength that would occur over the life of a larger structure, due to both small and large amplitude cyclic loads.

The experimental evidence in this paper provides impetus to challenge the conventional design paradigm of discounting undrained shear strength to allow for cyclic loading. Although a consolidation period is necessary for the observed strength gains to accumulate, they can be created by relatively low-level cyclic loading and offer potentially significant benefits in available bearing capacity.

ACKNOWLEDGEMENTS

This work was supported by the ARC Industrial Transformation Research Hub for Offshore Floating Facilities which is funded by the Australia Research Council, Woodside Energy, Shell, Bureau Veritas and Lloyds Register (Grant No. IH140100012). The third author acknowledges the support of the Shell Chair in Offshore Engineering at UWA.

NOTATION

c_h	coefficient of consolidation
D	diameter of T-bar
N	cycle number
$N_{\text{T-bar}}$	T-bar bearing factor
q	measured penetration resistance
q_i	initial penetration resistance
s_u	undrained shear strength
$s_{u,i}$	initial undrained shear strength
S_t	soil sensitivity
$\left(\frac{s_u}{\sigma'_{v0}}\right)_{NC}$	normally consolidated undrained strength ratio
t_c	consolidation time
v_p	penetration velocity
z	soil depth
σ'_{v0}	in situ geostatic effective stress
γ'	soil effective unit weight

REFERENCES

Andersen, K.H., Kleven, A. & Heien, D. (1988). Cyclic soil data for design of gravity structures. ASCE, *Journal of Geotechnical engineering* **114**, No. 5, 517–539.

Andersen, K.H. (2015). Cyclic soil parameters for offshore foundation design. In *Frontiers in Offshore Geotechnics–ISFOG III* (Ed. Meyer, V.), 3-82, Oslo, Norway, Taylor & Francis Group, London.

Bergaya, F., Theng, B., and Lagaly, G. (2006). Handbook of clay science. Elsevier, Amsterdam.

Chow, S.H., O'Loughlin, C.D., Zhou, Z., White, D.J. and Randolph, M.F. (2019). Penetrometer testing in a calcareous silt to explore changes in soil strength. To be submitted.

Cocjin M., Gourvenec S.M., White D.J. & Randolph M.F. (2017). Theoretical framework for predicting the response of tolerably mobile subsea installations. *Géotechnique*. **67**(7):608-620.

Colreavy, C., O'Loughlin, C.D., Bishop, D. T. and Randolph, M.F. (2019). Effect of soil biology and pore water chemistry on a lakebed sediment, *Géotechnique,* in press, doi: 10.1680/jgeot.16.P.308.

Hodder M. White D.J. & Cassidy M.J. (2013). An effective stress framework for the variation in penetration resistance due to episodes of remoulding and reconsolidation. *Géotechnique*, **63**(1):30-43.

Martin, C.M. and Randolph, M.F. (2006). Upper bound analysis of lateral pile capacity in cohesive soil. *Géotechnique*, **56**(2), 141-145.

Sahdi F., Boylan N., Gaudin C., &, White D.J. (2010). The influence of coloured dyes on the undrained shear strength of kaolin. *Int. Conf. on Physical Modelling in Geotechnics*. Zurich, Switzerland, 165-170.

Schneider M., Stanier S., White D.J. & Randolph M.F. (2019). Shallow penetrometer tests: theoretical and experimental modelling of the rotation stage. Submitted for publication.

Suzuki, Y. (2015). Investigation and interpretation of cone penetrometer rate effects. PhD thesis. The University of Western Australia.

White D.J. & Hodder M. (2010). A simple model for the effect on soil strength of remoulding and reconsolidation. *Canadian Geotechnical Journal*. 47:821-826.

White, DJ, Clukey EC, Randolph MF, Boylan NP, Bransby MF, Zakeri A, Hill AJ, Jaeck C. (2017). The state of knowledge of pipe-soil interaction for on-bottom pipeline design. *OTC 27623, Proc. Offshore Technology Conference*, Houston.

White D.J., Leckie, S.H.F., Draper, S., Zakarian, E. (2015). Temporal changes in pipeline-seabed condition and their effect on operating behaviour. *Proc. Int. Conf. Offshore Mech. and Arctic Engng*. OMAE2015-42216.

Zhou Z., White D.J. & O'Loughlin C.D. (2019). An effective stress framework for estimating penetration resistance accounting for changes in soil strength from maintained load, remoulding and reconsolidation. *Géotechnique* **69**(1):57-71.

1. FIGURE CAPTIONS

2. TABLE CAPTIONS

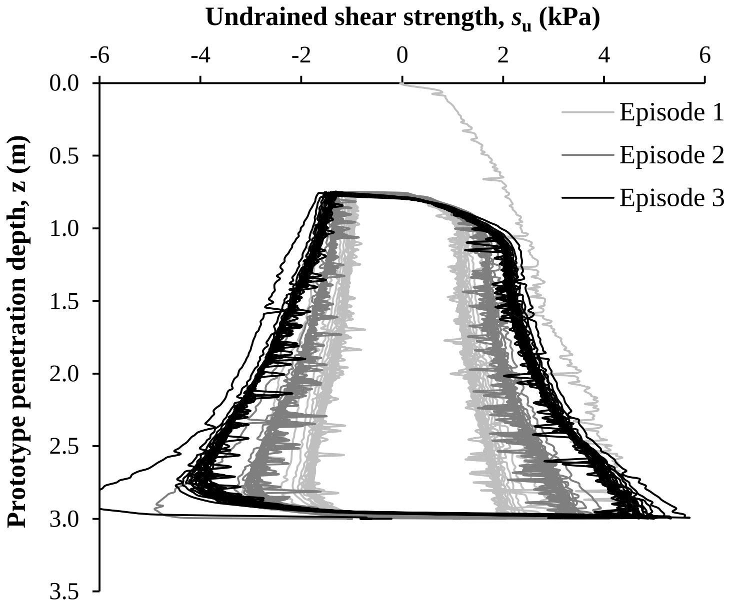

(a)

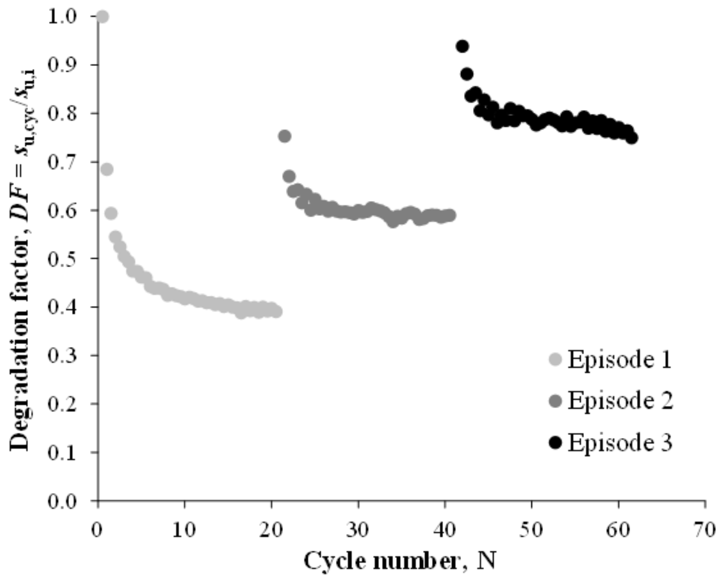

(b)

Figure 1 Changing soil strength due to cyclic remoulding and reconsolidation (after Hodder et al. 2013).

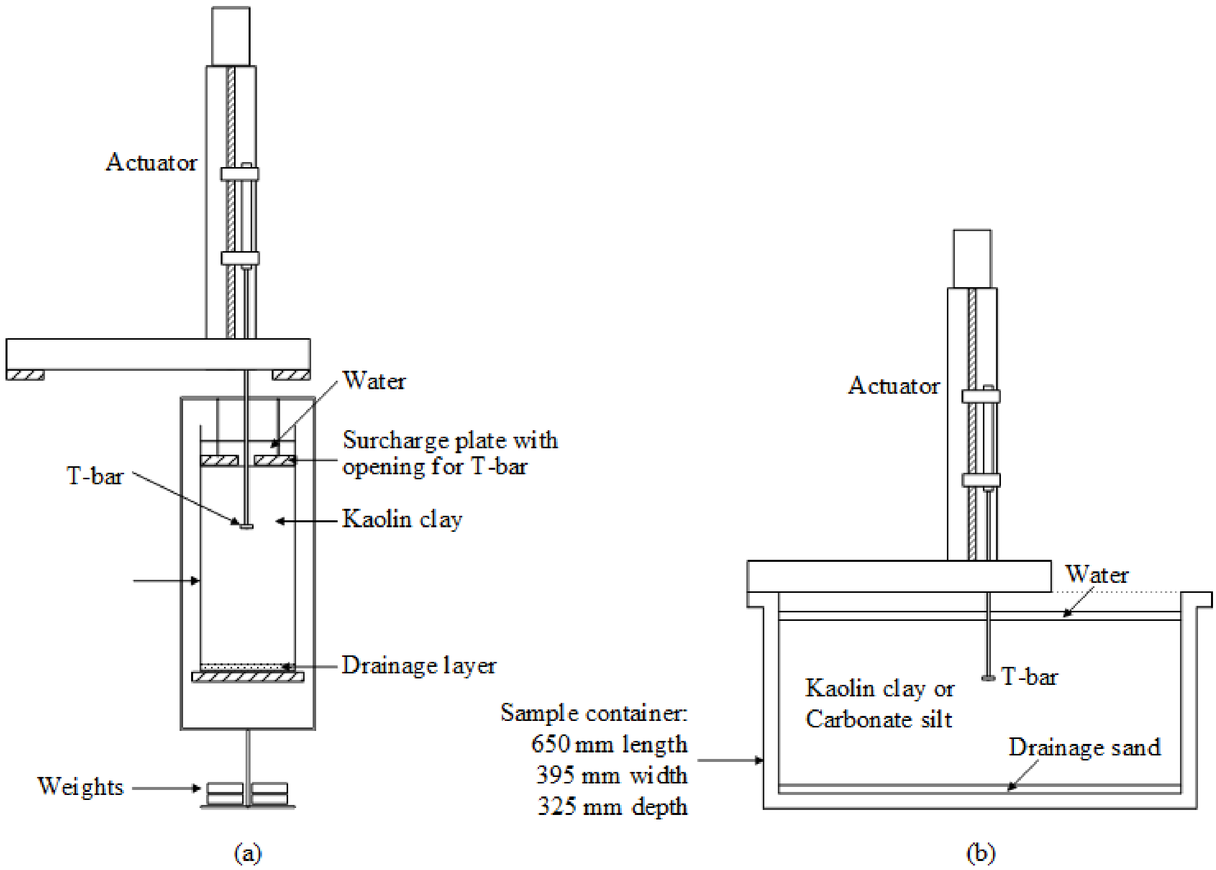

Figure 2 Experimental arrangement: (a) single gravity tests, (b) centrifuge tests.

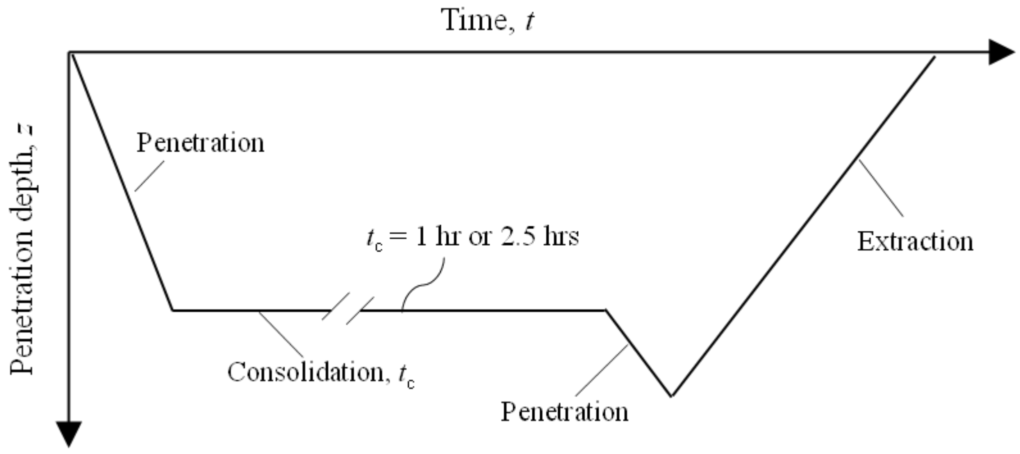
Time, t
Penetration depth, z
Penetration
t_c = 1 hr or 2.5 hrs
Extraction
Consolidation, t_c
Penetration

(a)

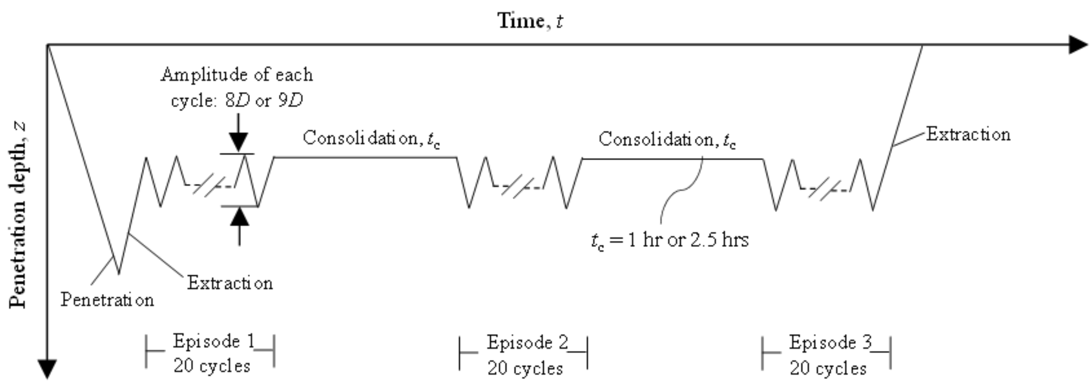
Time, t
Penetration depth, z
Amplitude of each cycle: 8D or 9D
Consolidation, t_c
Consolidation, t_c
Extraction
t_c = 1 hr or 2.5 hrs
Penetration
Extraction
Episode 1
20 cycles
Episode 2
20 cycles
Episode 3
20 cycles

(b)

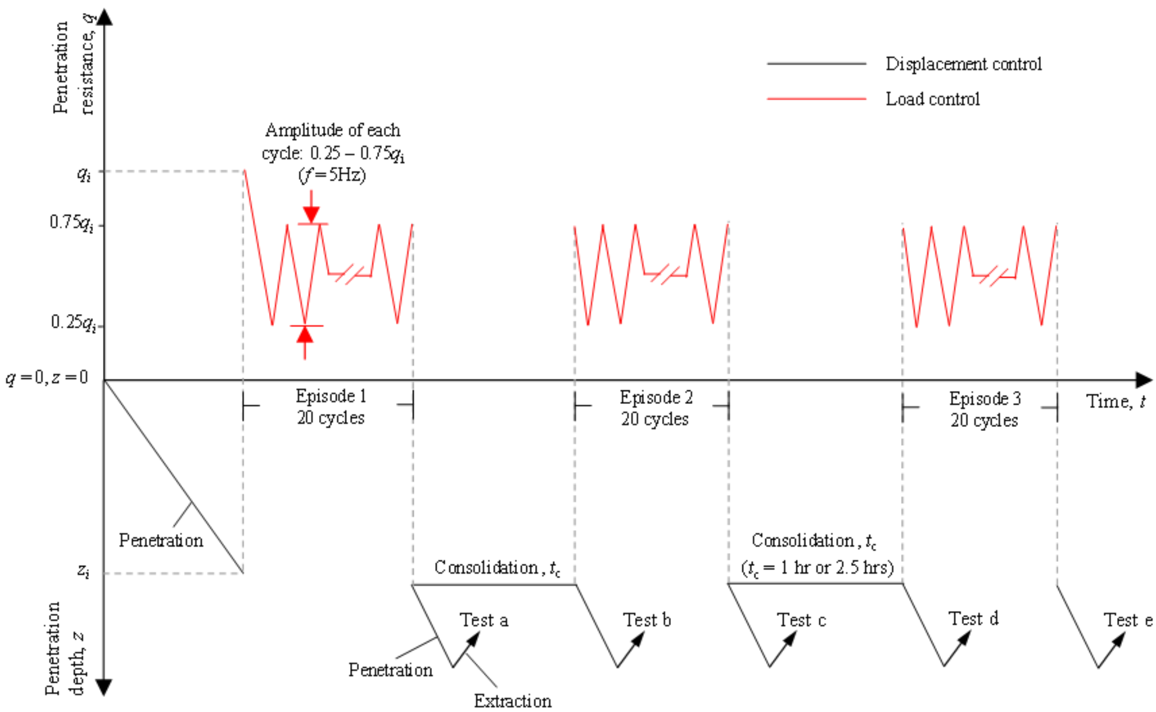
Penetration resistance, q
Displacement control
Load control
Amplitude of each cycle: 0.25 – 0.75q_i
(f=5Hz)
q_i
0.75q_i
0.25q_i
q = 0, z = 0
Episode 1
20 cycles
Episode 2
20 cycles
Episode 3
20 cycles
Time, t
Penetration
z_i
Consolidation, t_c
Consolidation, t_c
(t_c = 1 hr or 2.5 hrs)
Test a
Test b
Test c
Test d
Test e
Penetration
Extraction
Penetration depth, z

(c)

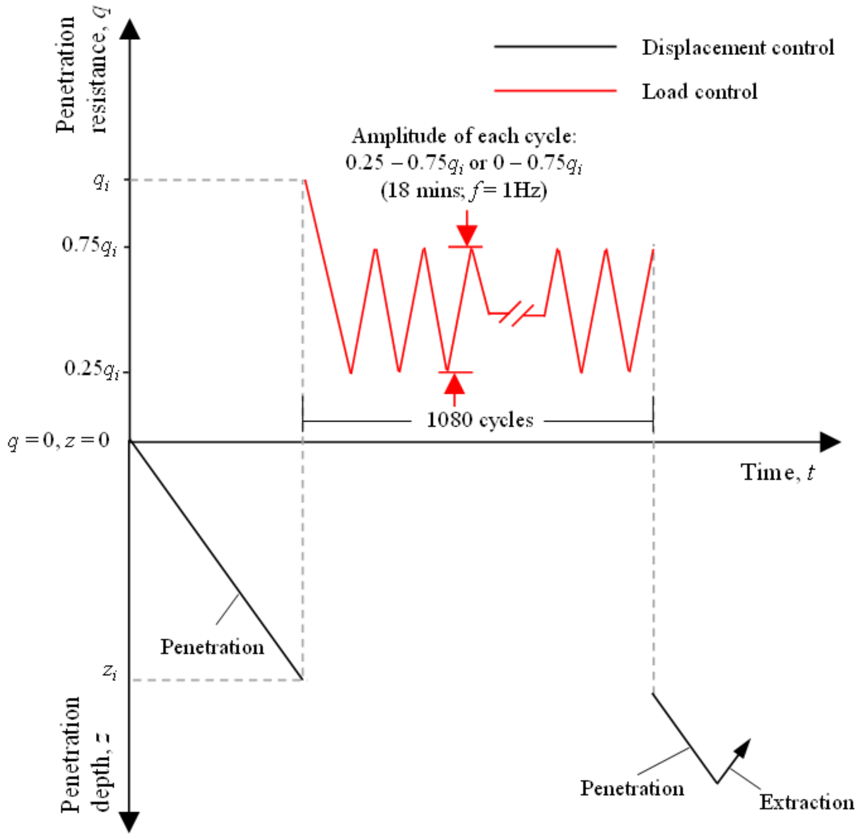

(d)

Figure 3 Test procedures: (a) Type I, (b) Type II, (c) Type III, (d) Type IV

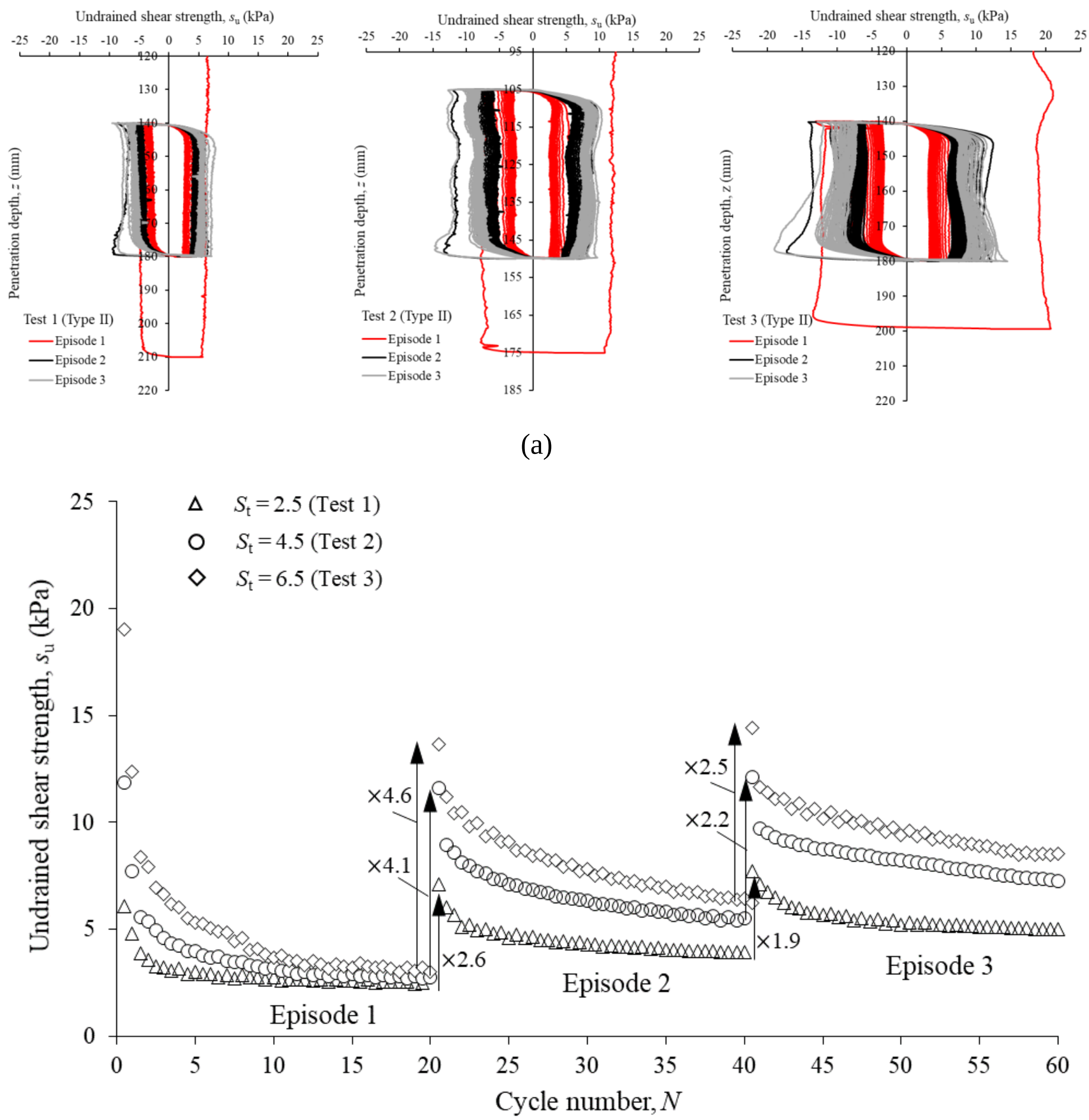

(a)

(b)

Figure 4 Single gravity test results: displacement controlled cycles (Test Type II): (a) undrained shear strength profiles, (b) Change in undrained shear strength during cycles and after consolidation periods

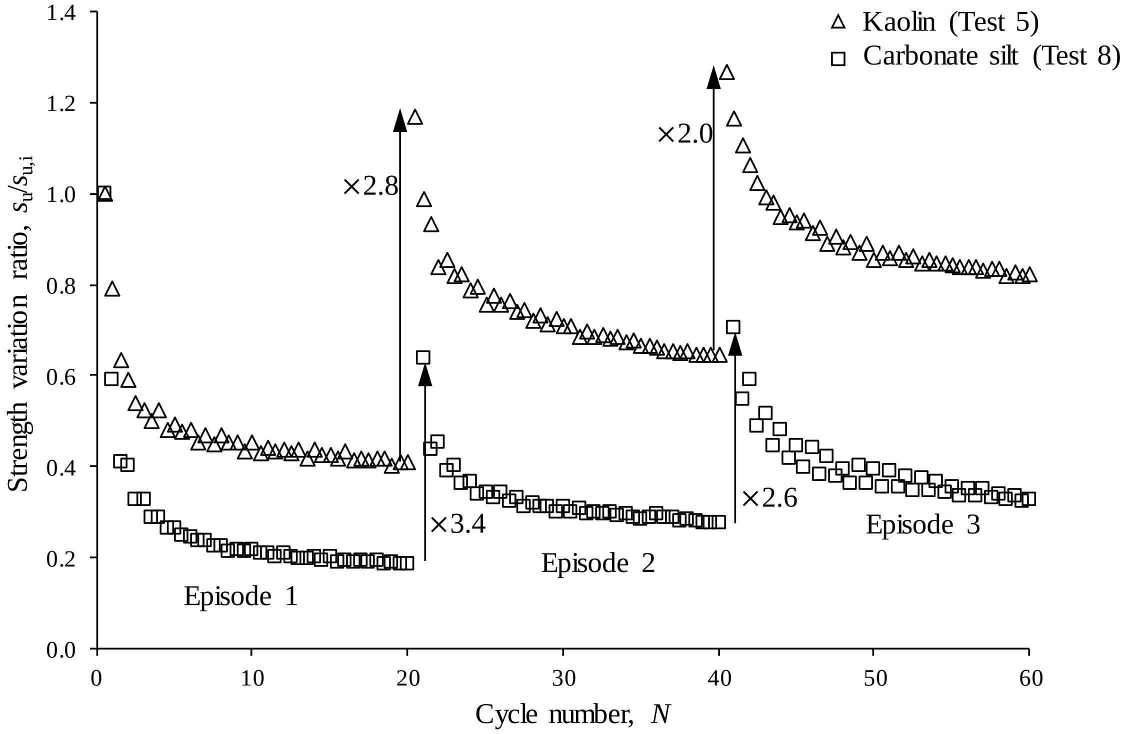

Figure 5 Comparison of changing soil strength due to remoulding (displacement controlled cycles, Test type II (centrifuge)) and reconsolidation in carbonate silt and kaolin clay

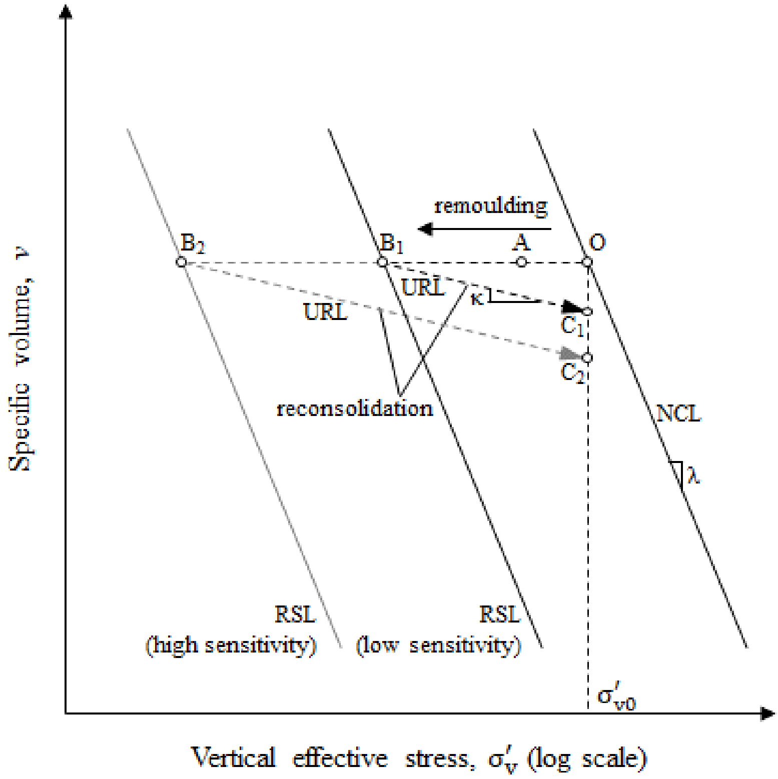

Figure 6 Effective stress path for Test type II (single gravity tests)

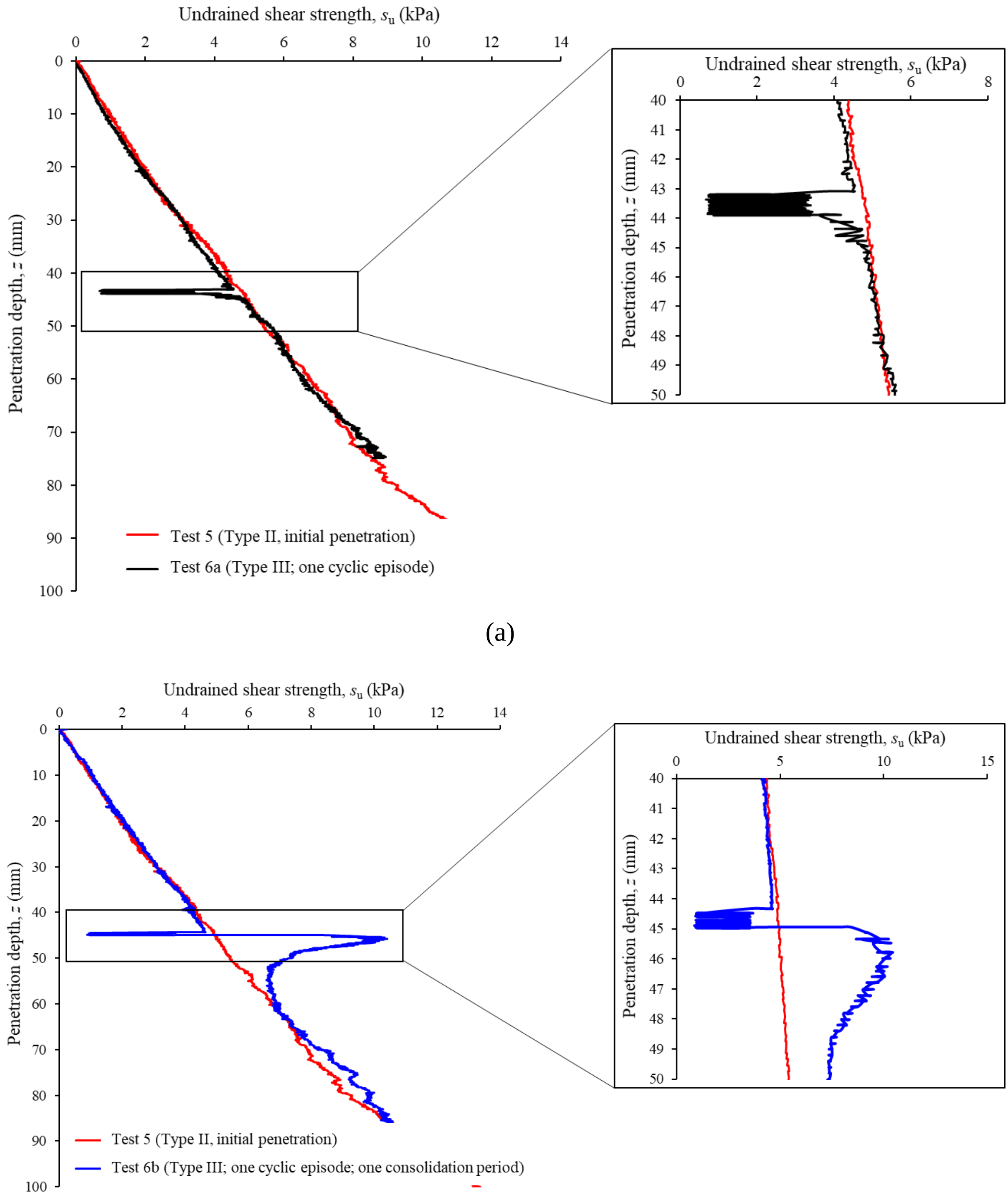

Figure 7 Example results from load-controlled T-bar tests (centrifuge) in kaolin clay: (a) cyclic loading, (b) cyclic loading followed by a consolidation period

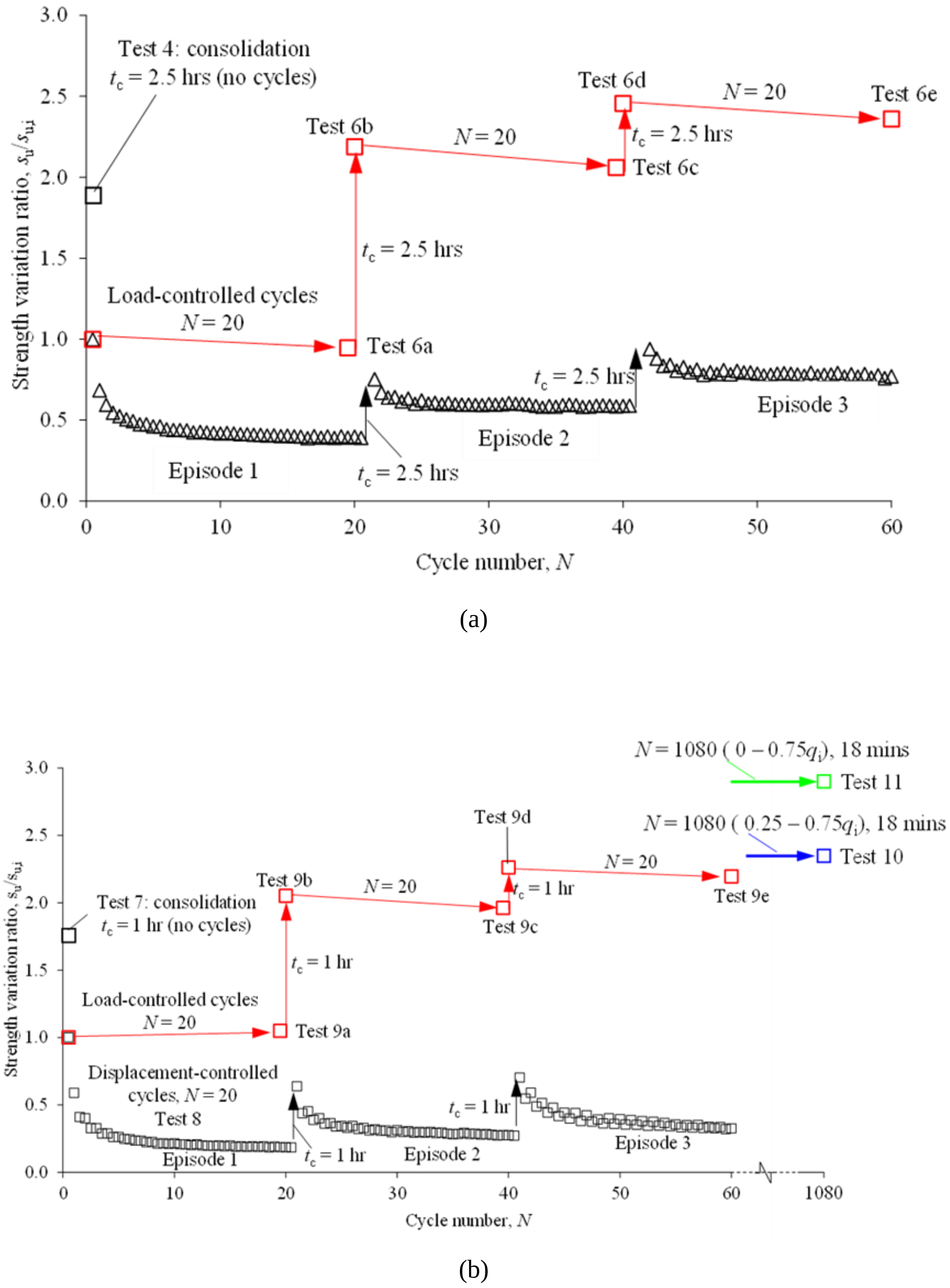

Figure 8 Comparison of changing soil strength due to load and displacement controlled loading cycles in the centrifuge tests: (a) kaolin clay, (b) carbonate silt

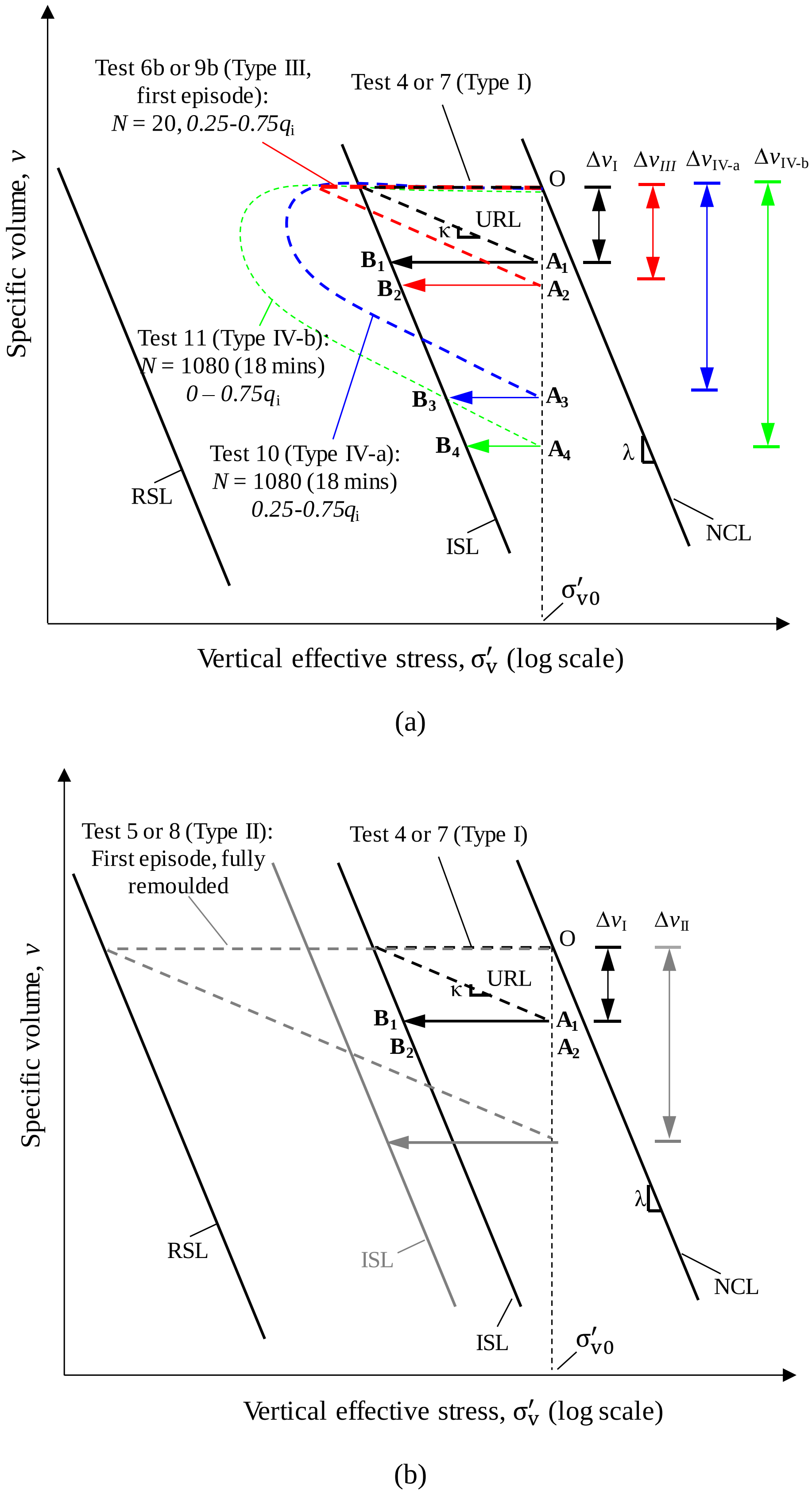

Figure 9 Effective stress paths for: (a) load controlled cyclic T-bar tests, (b) displacement- and load-controlled T-bar tests.

Table 1 Soil parameters

Soil properties	Kaolin clay	Carbonate silt
Specific gravity, G_s	2.6	2.71
Liquid limit, LL (%)	61	67
Plastic limit, PL (%)	27	39
Compression index, λ	0.205	0.287
Swelling index, κ	0.044	0.036
Soil sensitivity, S_t	2.5, 4.5, 6.5	5
Normally consolidated undrained strength ratio, $(s_u/\sigma'_{v0})_{NC}$	0.15 (S_t = 2.5) 0.25 (S_t = 4.5)[*] 0.40 (S_t = 6.5)[**]	0.385
Coefficient of horizontal consolidation, c_h (m^2/year)	2.6 (σ'_v = 40 kPa)	8.9 (σ'_v = 40 kPa)

[*]: Batch 1 (S_t = 4.5): 5 kg of kaolin powder mixed with (a) flocculant: 0.1 kg Sodium Hexametaphosphate dissolved in 2.5 kg water; and (b) dispersant: 0.0005 kg Sodium Polyacrylate dissolved in 2.5 kg water.

[**]: Batch 2 (S_t = 6.5): 5 kg of kaolin powder mixed with (a) flocculant: 0.1 kg Sodium Hexametaphosphate dissolved in 2.5 kg water; and (b) dispersant: 0.00075 kg Sodium Polyacrylate dissolved in 2.5 kg water.

Table 2 Test parameters

Test environment	Soil type	Test no.	Soil sensitivity	Test type	Test parameters
Single gravity	Kaolin clay	Test 1	2.5	Type II	t_c = 24 hrs
		Test 2	4.5		t_c = 24 hrs
		Test 3	6.5		t_c = 24 hrs
Centrifuge	Kaolin clay	Test 4	2.5	Type I	t_c = 2.5 hrs
		Test 5		Type II	t_c = 2.5 hrs
		Test 6a		Type III	-
		Test 6b			t_c = 2.5 hrs
		Test 6c			
		Test 6d			
		Test 6e			
	Carbonate silt	Test 7	5	Type I	t_c = 1 hr
		Test 8		Type II	t_c = 1 hr
		Test 9a		Type III	-
		Test 9b			t_c = 1 hr
		Test 9c			
		Test 9d			
		Test 9e			
		Test 10		Type IV	Cyclic loading: $0.25q_i – 0.75q_i$
		Test 11		Type IV	Cyclic loading: $0 – 0.75q_i$

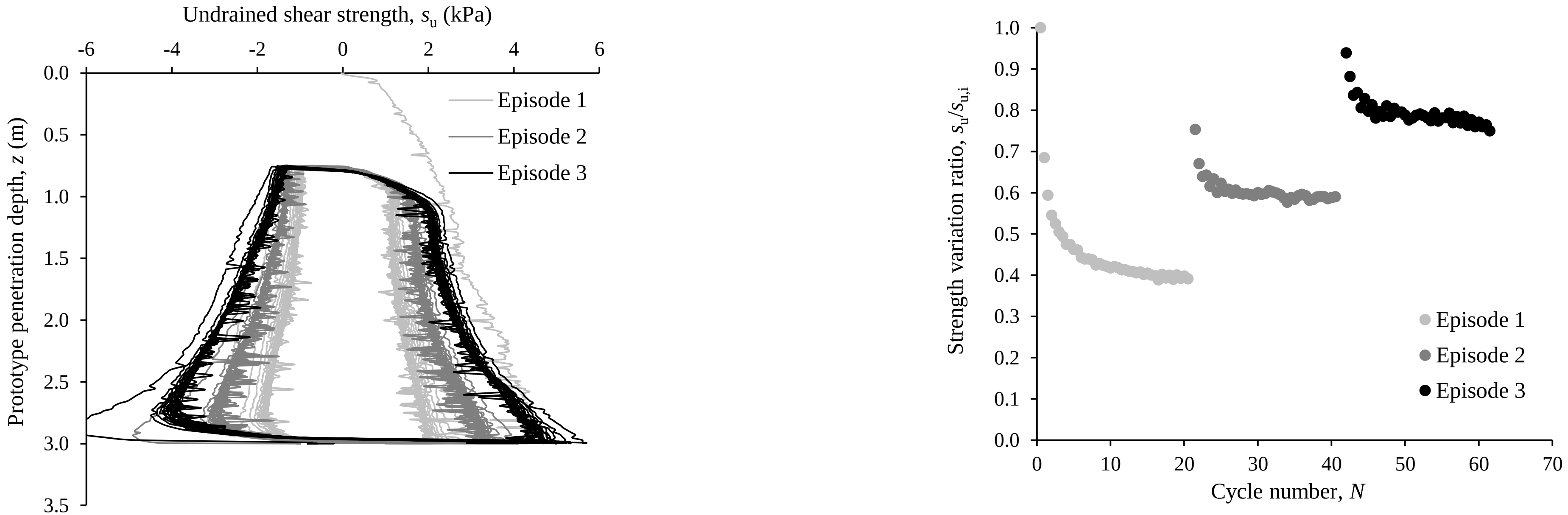

Figure 1 Changing soil strength due to cyclic remoulding and reconsolidation (after Hodder et al. 2013).

Figure 2

Click here to access/download;Figure;OLoughlinfig02.pptx

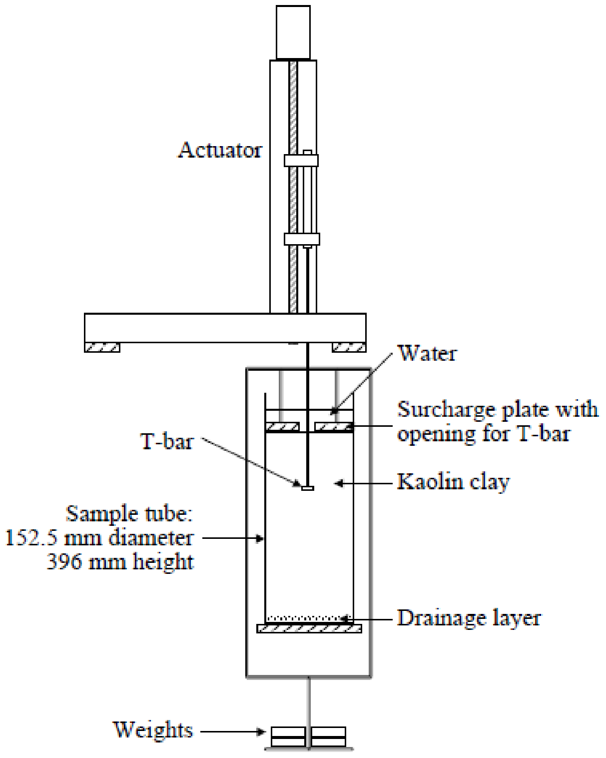

(a)

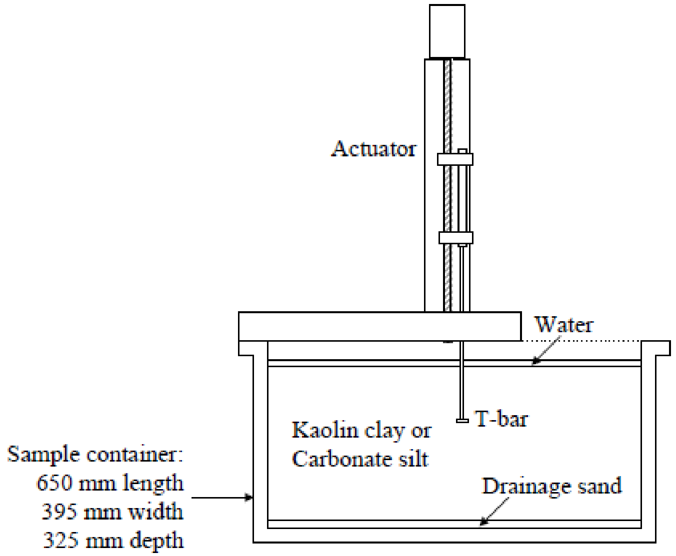

(b)

Figure 3

Click here to access/download;Figure;OLoughlinfig03.pptx

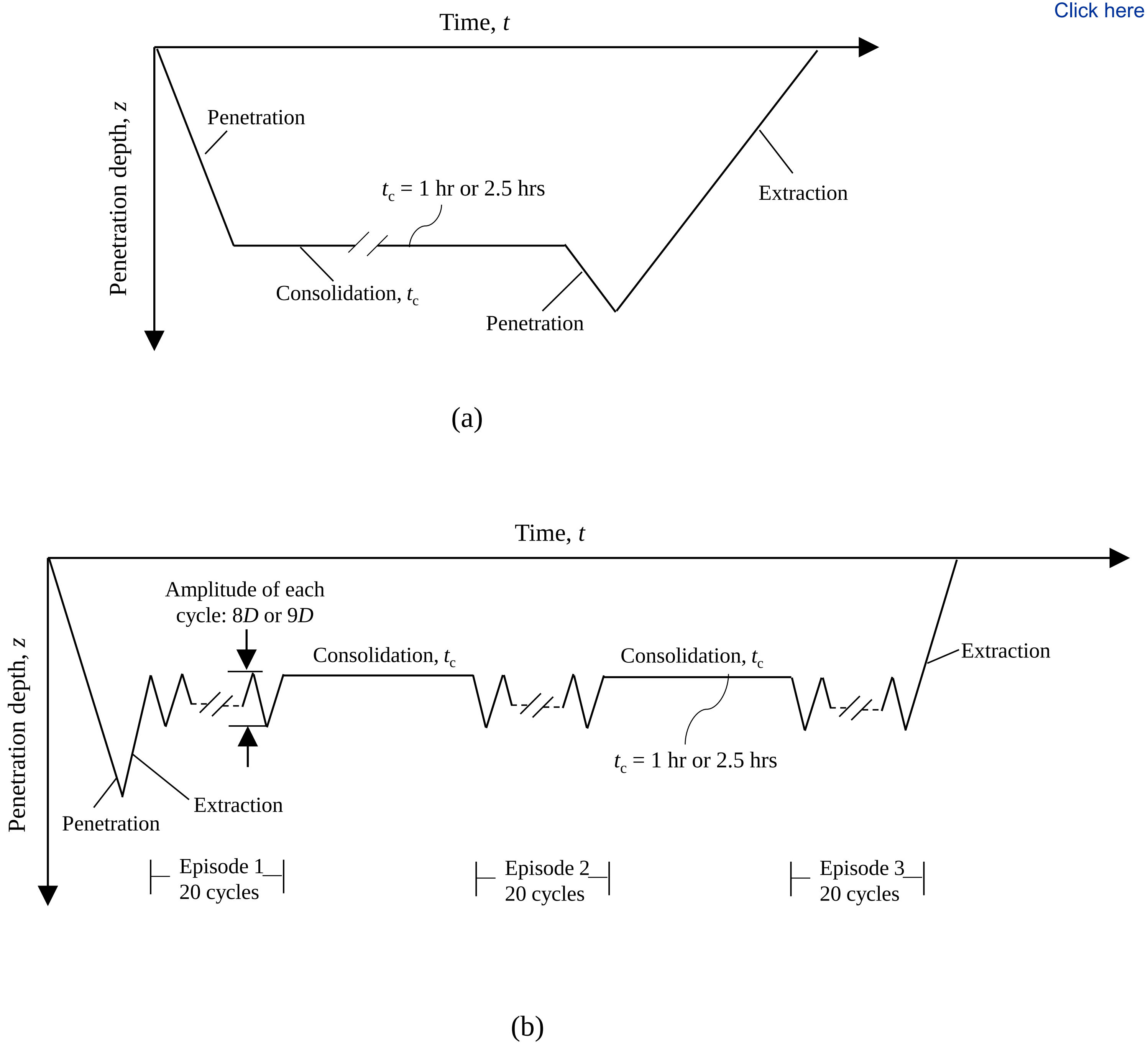

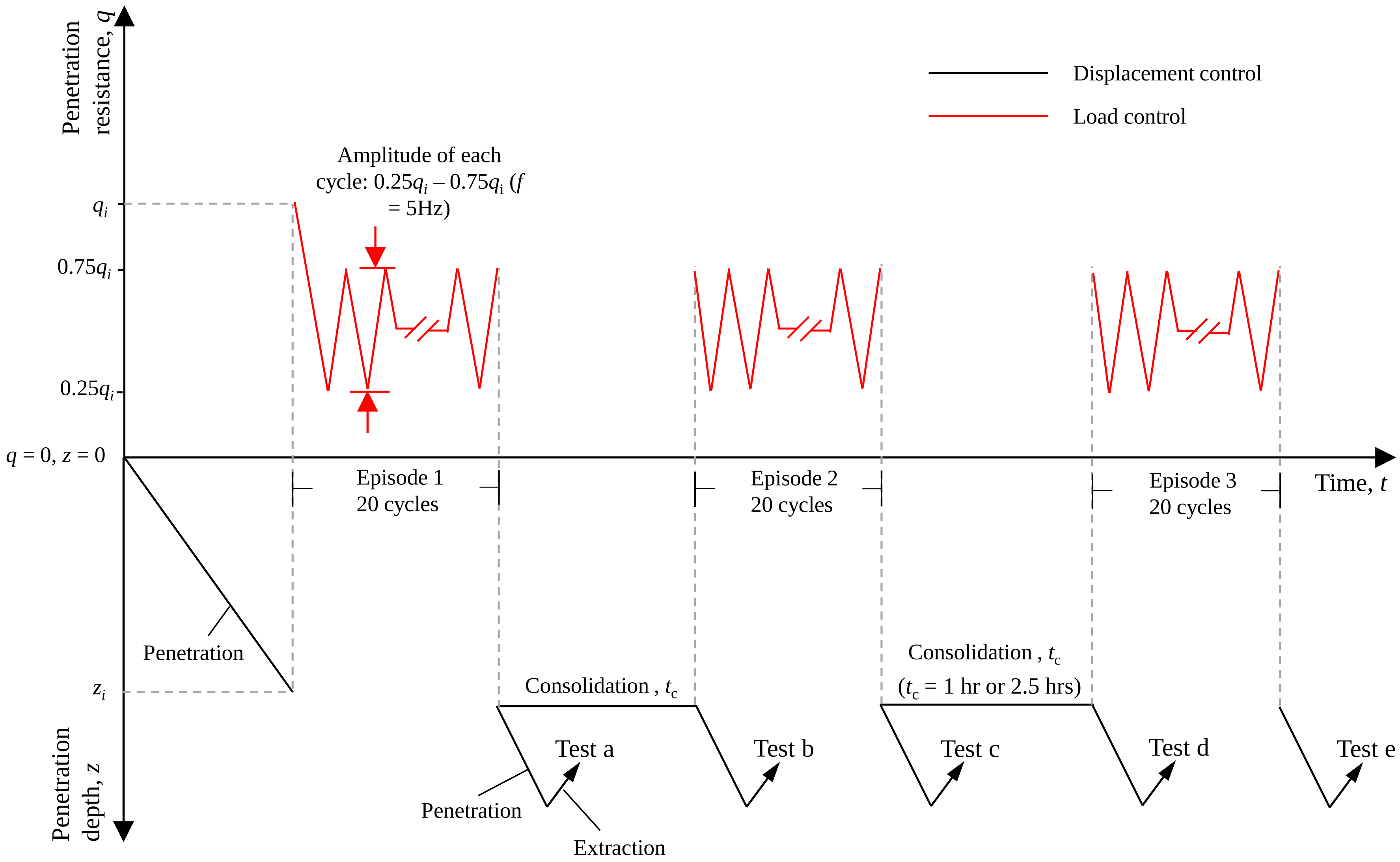
Penetration resistance, q
Displacement control
Load control
Amplitude of each cycle: 0.25q_i – 0.75q_i (f = 5Hz)
q_i
0.75q_i
0.25q_i
q = 0, z = 0
Episode 1
20 cycles
Episode 2
20 cycles
Episode 3
20 cycles
Time, t
Penetration
z_i
Consolidation , t_c
Consolidation , t_c
(t_c = 1 hr or 2.5 hrs)
Test a
Test b
Test c
Test d
Test e
Penetration
Extraction
Penetration depth, z

(c)

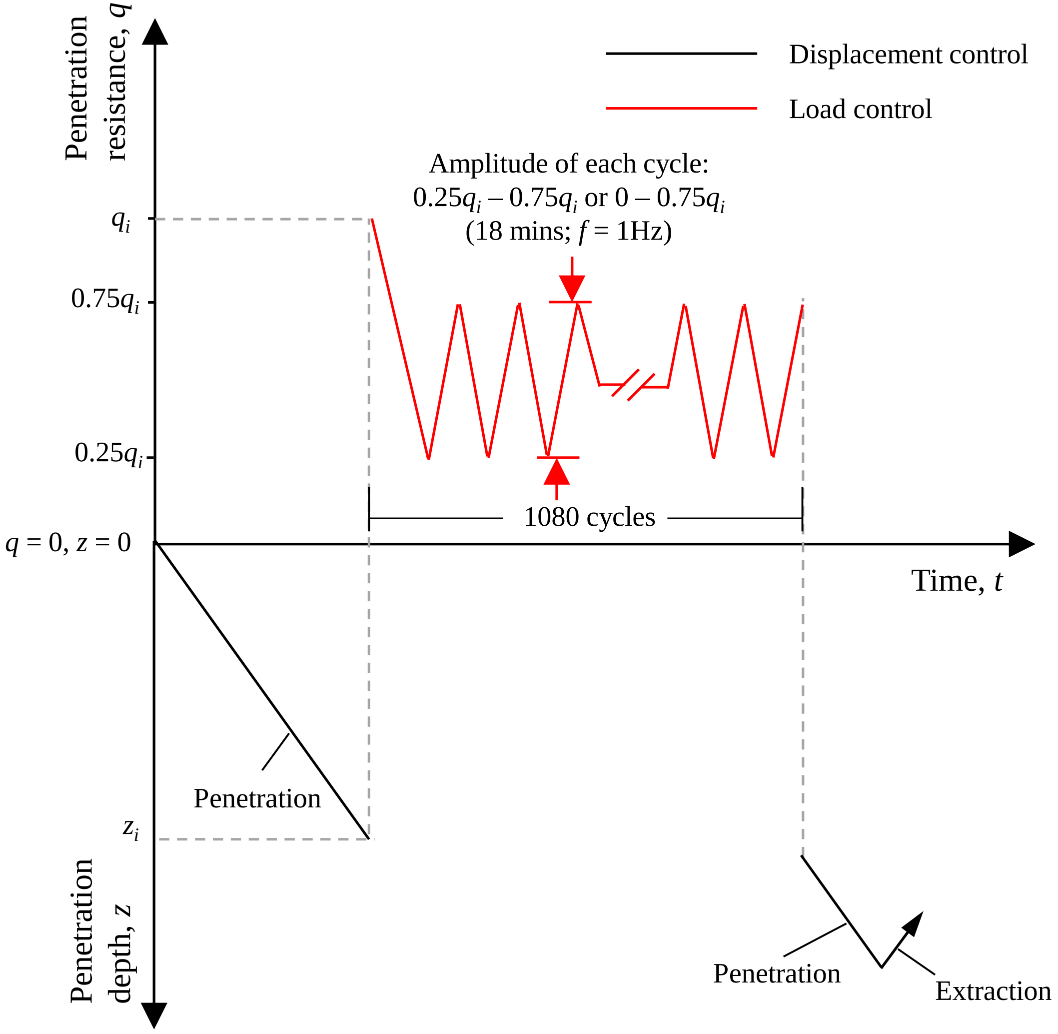

Penetration resistance, q
Displacement control
Load control
Amplitude of each cycle:
0.25qi – 0.75qi or 0 – 0.75qi
(18 mins; f = 1Hz)
qi
0.75qi
0.25qi
1080 cycles
q = 0, z = 0
Time, t
Penetration
zi
Penetration depth, z
Penetration
Extraction

(d)

Figure 4

Click here to access/download;Figure;OLoughlinfig04.pptx

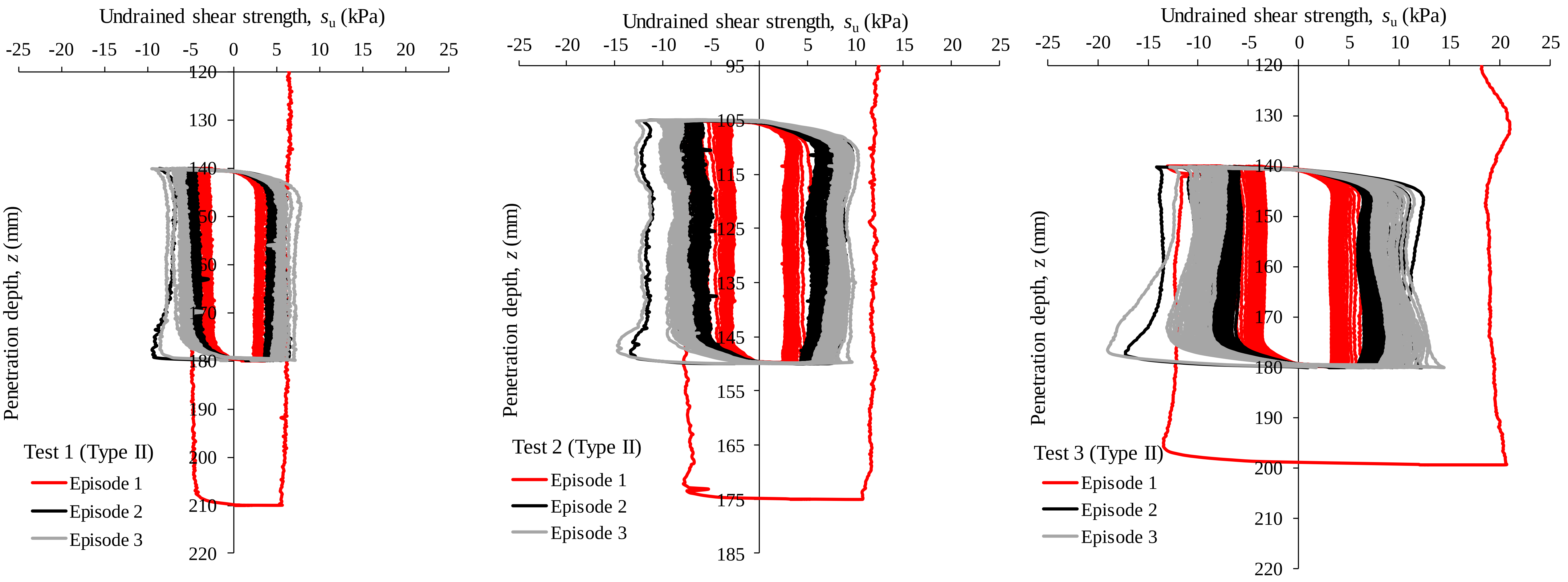

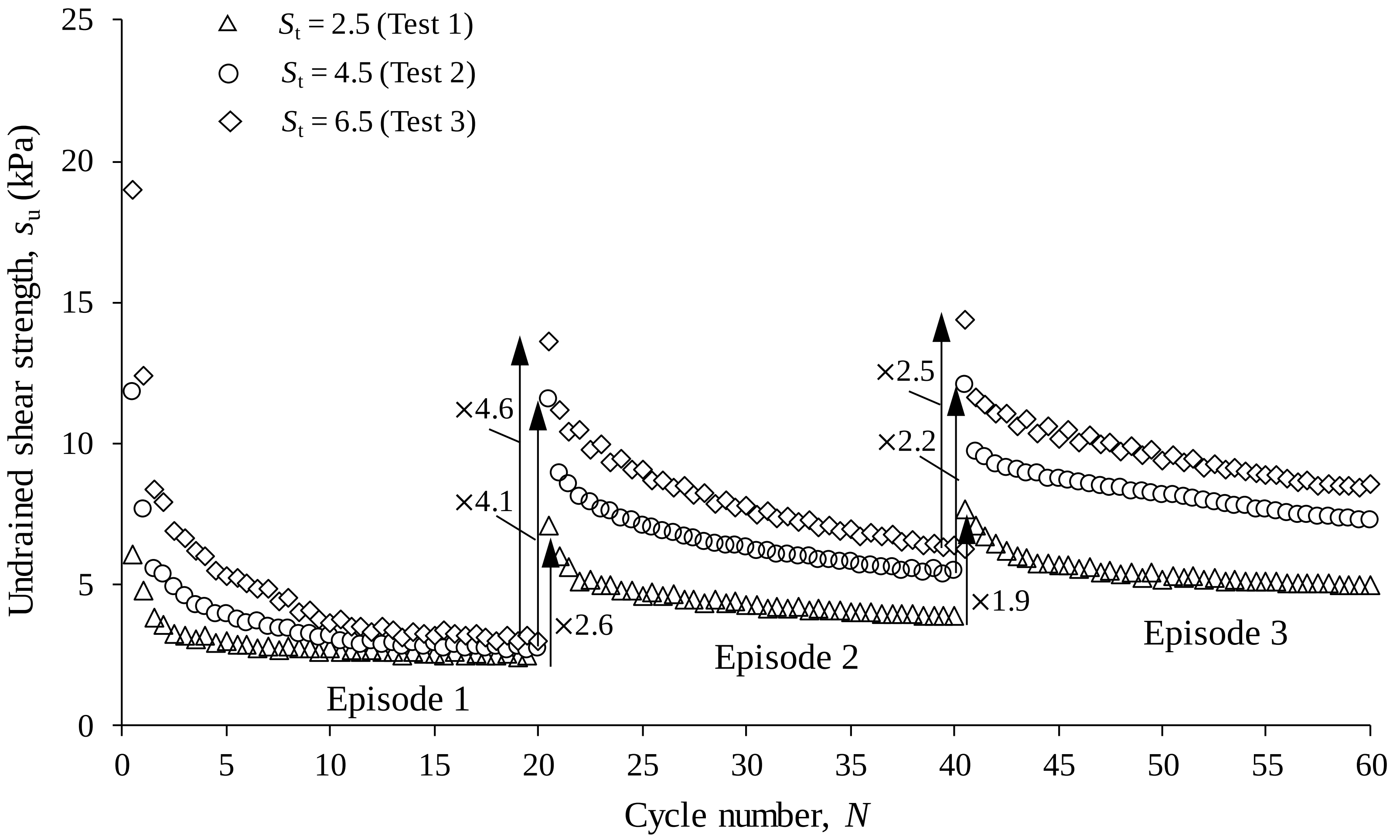

S_t = 2.5 (Test 1)
S_t = 4.5 (Test 2)
S_t = 6.5 (Test 3)
Undrained shear strength, s_u (kPa)
Cycle number, N
0
5
10
15
20
25
0
5
10
15
20
25
30
35
40
45
50
55
60
×4.6
×4.1
×2.6
×2.5
×2.2
×1.9
Episode 1
Episode 2
Episode 3

Figure 5

Click here to access/download;Figure;OLoughlinfig05.pptx

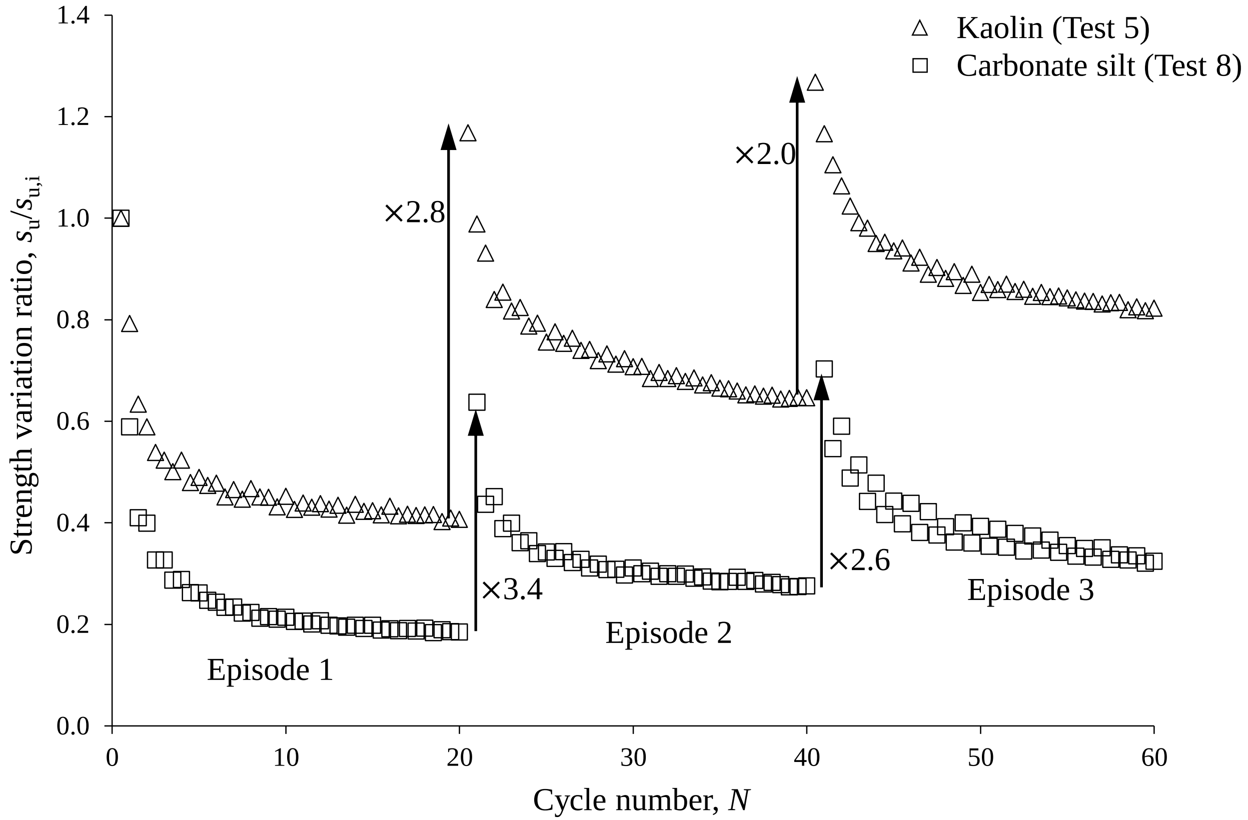

Figure 6

Click here to access/download;Figure;OLoughlinfig06.pptx

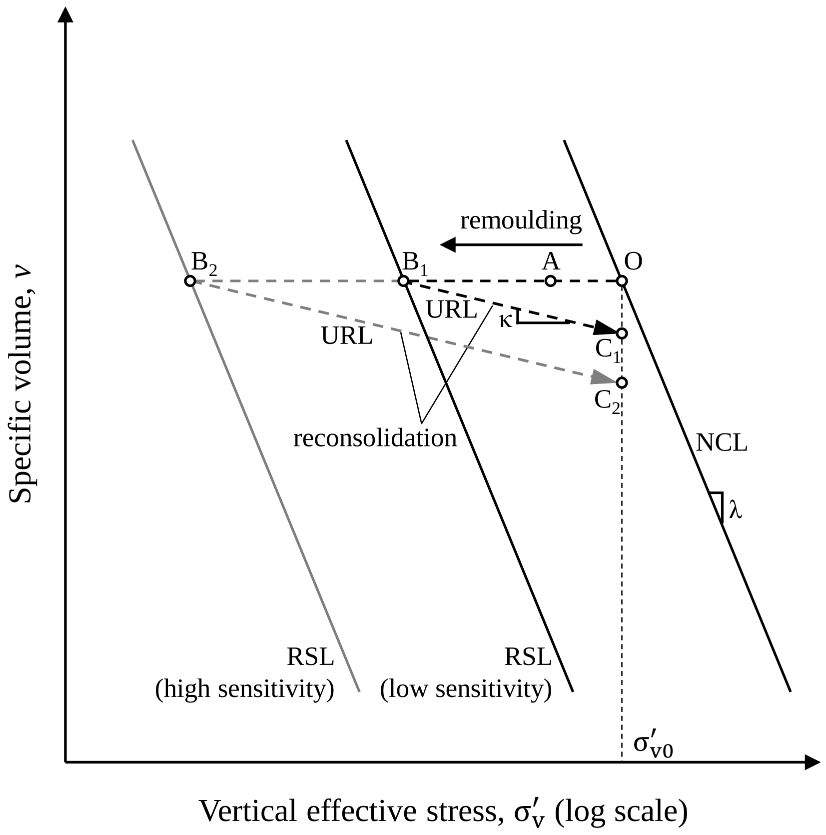

Figure 7

Click here to access/download;Figure;OLoughlinfig07.pptx

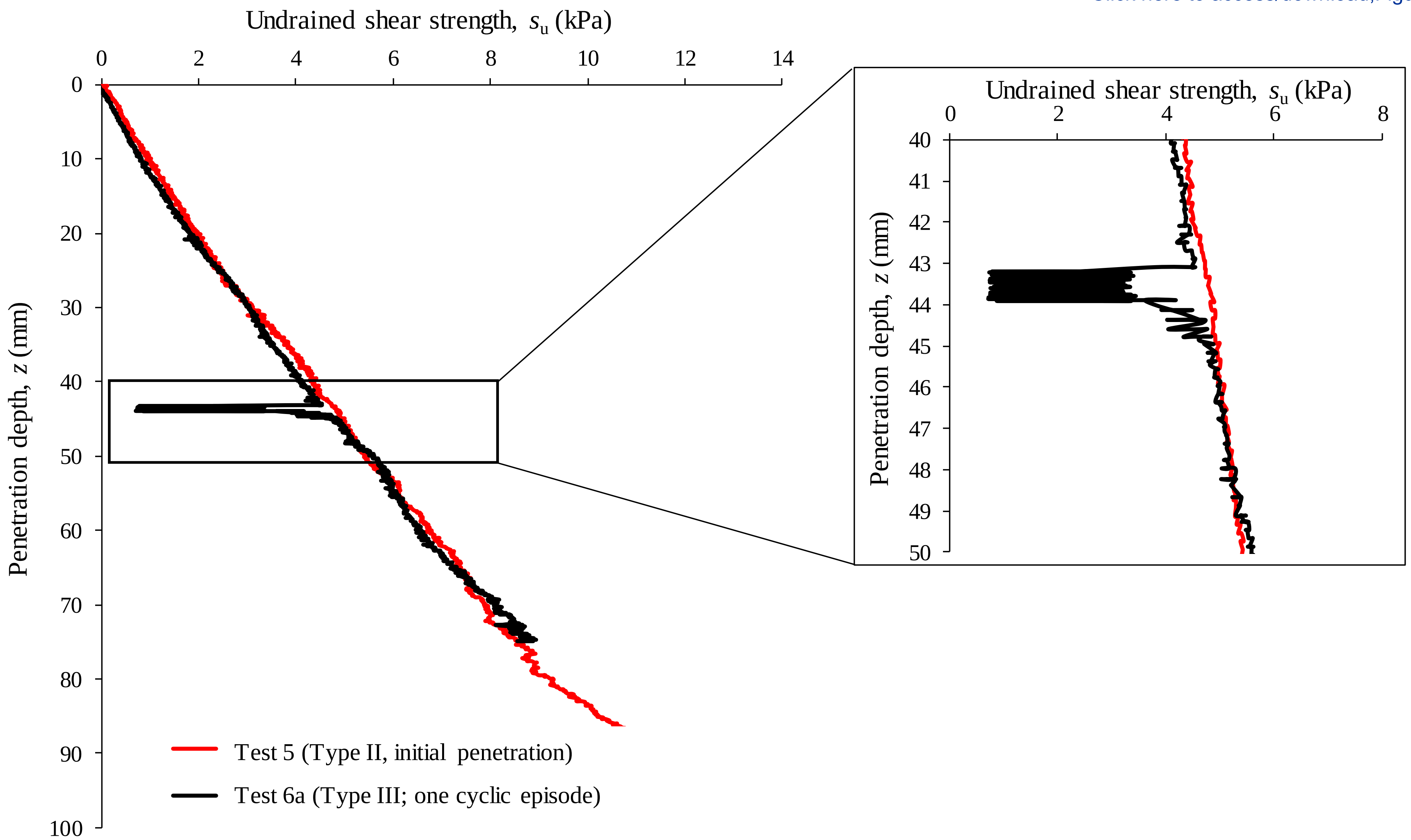

(a)

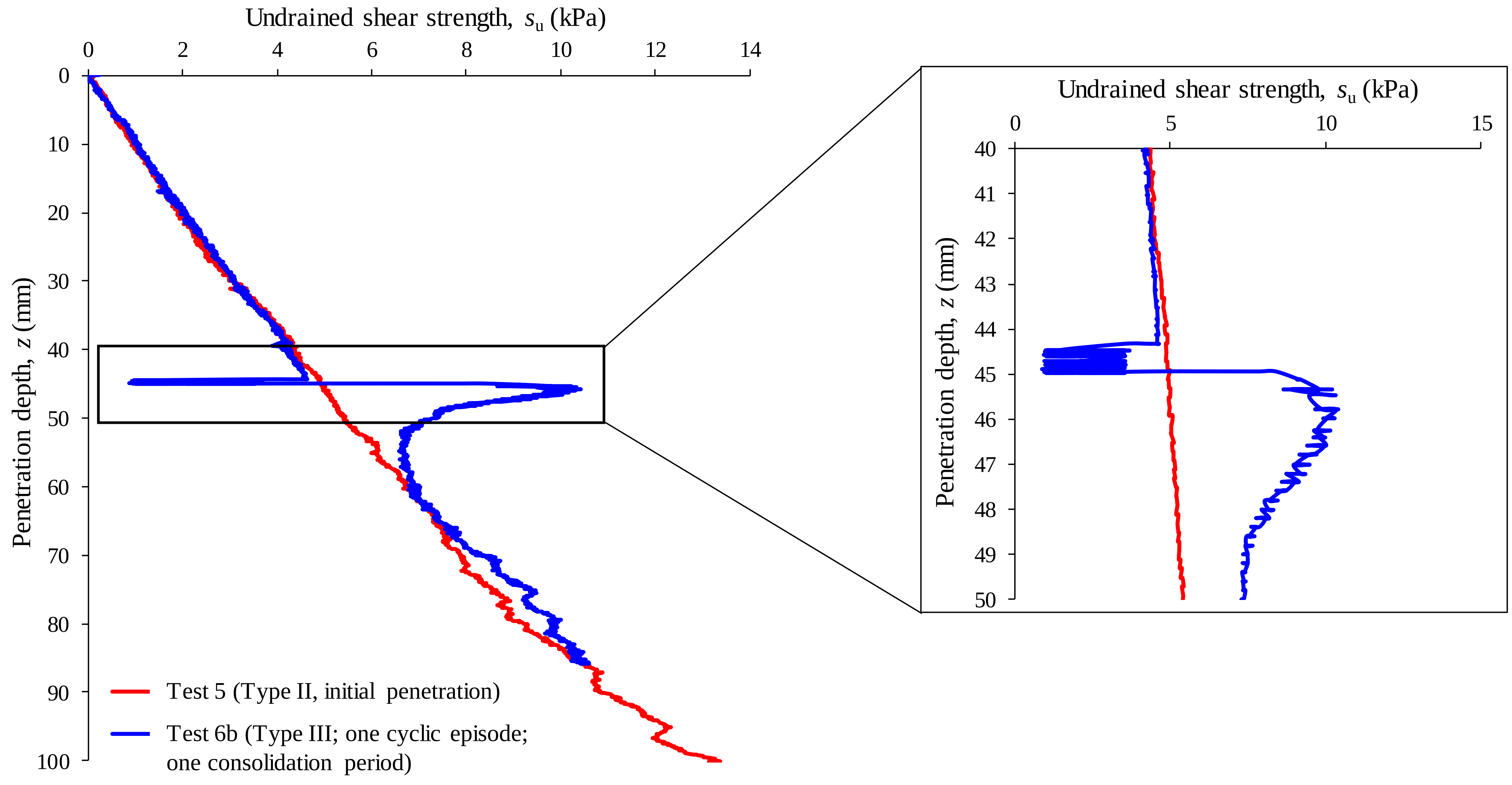

Undrained shear strength, s_u (kPa)
0
2
4
6
8
10
12
14
0
10
20
30
40
50
60
70
80
90
100
Penetration depth, z (mm)
Test 5 (Type II, initial penetration)
Test 6b (Type III; one cyclic episode; one consolidation period)
Undrained shear strength, s_u (kPa)
0
5
10
15
40
41
42
43
44
45
46
47
48
49
50
Penetration depth, z (mm)

(b)

Figure 8

Click here to access/download;Figure;OLoughlinfig08.pptx

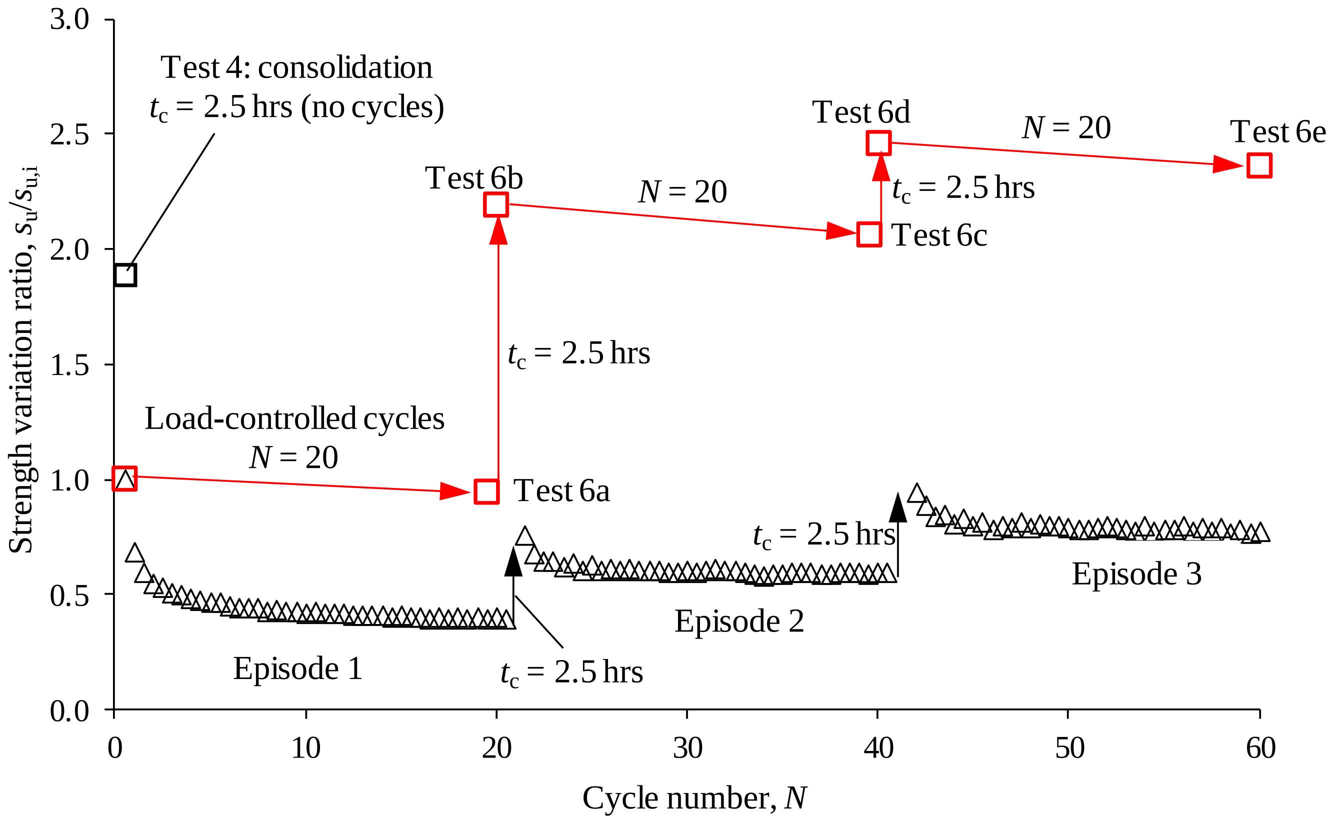

(a)

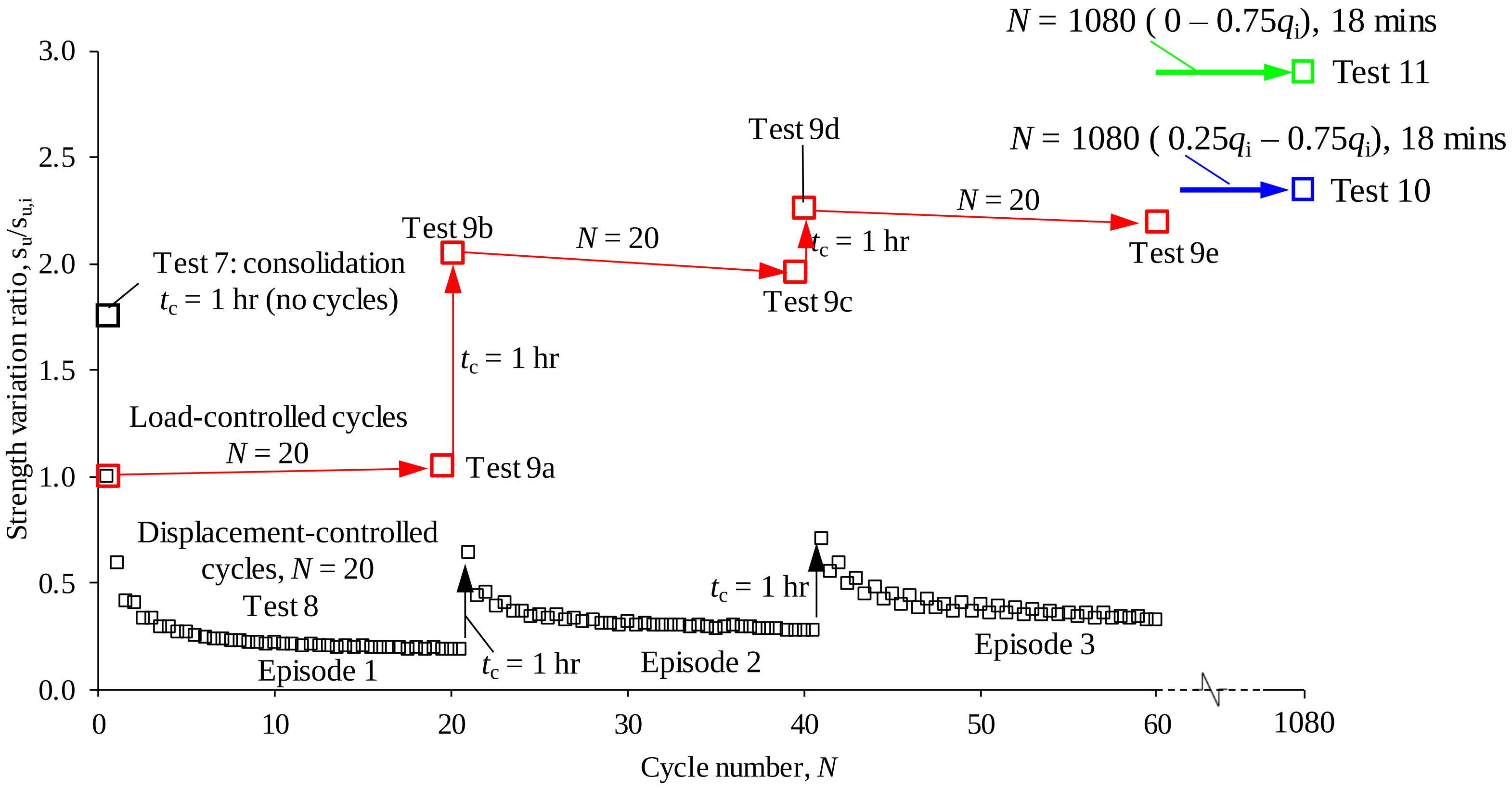
N = 1080 (0 – 0.75qi), 18 mins
Test 11
N = 1080 (0.25qi – 0.75qi), 18 mins
Test 10
Test 9d
Test 9b
N = 20
N = 20
tc = 1 hr
Test 9e
Test 9c
Test 7: consolidation
tc = 1 hr (no cycles)
tc = 1 hr
Load-controlled cycles
N = 20
Test 9a
Displacement-controlled
cycles, N = 20
Test 8
tc = 1 hr
tc = 1 hr
Episode 1
Episode 2
Episode 3
Strength variation ratio, su/su,i
Cycle number, N
3.0
2.5
2.0
1.5
1.0
0.5
0.0
0
10
20
30
40
50
60
1080

(b)

Figure 9

Click here to access/download;Figure;OLoughlinfig09.pptx